Lamellar to Columnar Mesophase Evolution in a Series of PAMAM Liquid-Crystalline Codendrimers

Jean-Michel Rueff,[†] Joaquín Barberá,[†] Bertrand Donnio,[‡] Daniel Guillon,[‡,§] Mercedes Marcos,[†] and José-Luis Serrano*[,†,⊥]

Química Orgánica-Dpto. Nuevos Materiales Orgánicos, Facultad de Ciencias-Instituto de Ciencia de Materiales de Aragón, Universidad de Zaragoza-CSIC, E-50009 Zaragoza, Spain, and Groupe des Matériaux Organiques, Institut de Physique et Chimie des Matériaux de Strasbourg, UMR 7504, 23, rue du Læss, BP 43, F-67034 Strasbourg Cedex 2, France

Received April 14, 2003; Revised Manuscript Received August 7, 2003

ABSTRACT: The synthesis, chemical characterization and liquid crystalline behavior of a series of seven poly(amidoamine) (PAMAM) codendrimers are described. These compounds were obtained by grafting two types of terminal promesogenic units, that carry either one or two decyloxy chains, in various proportions onto the third generation of PAMAM dendrimer. The average number of promesogenic units was determined by using an original interpretation of the NMR spectra. X-ray diffraction studies show that these compounds exhibit lamellar and/or columnar mesophases. The type of mesophase is determined by the number of each kind of promesogenic units present in a given codendrimer and by the temperature. The evolution of the supramolecular organization of the different molecules is explained as a function of the number of alkoxy chains present around the dendritic core and compared to the models developed for the homodendrimers totally functionalized by promesogenic units with either one or two decyloxy chains.

Introduction

One fascinating aspect of polymer chemistry is to observe how very weak intermolecular forces can determine the unique properties of these materials. Dendrimeric compounds,[1] a representative subclass of polymers, represent an optimum testing bench in these types of studies. In these covalent materials, the molecules are forced to adopt very constrained and regular structures, and consequently, the different molecular parts tend to look for the most favorable arrangement in order to generate the most stable structure.

In liquid crystalline dendrimers,[2] the interactions between the different mesogenic units can modify to a great extent the molecular arrangement and consequently the type of mesophase observed. Moreover, liquid crystalline dendrimers are also of academic interest in that they combine two opposite tendencies within the same molecule: an isotropic dendritic architecture to which anisotropic structural units are attached. This particular block may behave in two opposite ways depending on the balance between the dendritic part and the anisotropic units part. Either the dendritic branches radiate from a central core, becoming more crowded as they extend out to the periphery (this results in a spherical morphology (starburst shape in dendrimer terminology) where all the branches are distributed isotropically in space because of entropic forces) or the mesogenic groups, showing strong anisotropic interactions between each other, tend to be oriented parallel to one another, resulting in the formation of mesophases driven by the enthalpic gain. Therefore, this class of materials represents a nice example of the competition between entropy and enthalpy within one single molecule.

The liquid crystalline properties of some poly(amidoamine) (PAMAM) dendrimers for which the terminal groups are functionalized by one-chain promesogenic calamitic units have been recently reported.[3] The geometry adopted by these compounds is completely different to the starburst structure adopted by the "naked" dendrimers i.e., dendrimers that do not contain any mesogenic groups on their outer surface. The weak interactions between the mesogenic units are strong enough to force the dendritic molecules into a cylindrical geometry, which resembles a heavy thick rodlike structure. As such, smectic and particularly SmA phases are formed by the mutual lateral arrangement of these giant rods.

Interestingly, hexagonal columnar phases have been obtained in an homologous series of the same dendrimers but with the promesogenic calamitic units functionalized by two or three terminal chains.[4] The various generations of dendrimers have been shown to adopt wedgelike or disk structures capable of self-organization into columnar supramolecular structures, by the self-assembling of these basic molecular objects into columns.

In contrast to what has been claimed of a series of carbosilane homodendrimers,[5] a direct transition between these two mesophases as a function of either the generation or the temperature has not yet been observed within this familly of dendrimers. It was therefore of particular interest to design new dendritic molecules that can show a lamellar to columnar mesophase transition within the same compound as a function of temperature. For this purpose, codendrimers functionalized by two different promesogenic units bearing one or two terminal aliphatic chains respectively, have been prepared. In this paper we present the results obtained from a series of homologous, third generation, PAMAM

[†] Universidad de Zaragoza-CSIC.
[‡] Institut de Physique et Chimie des Matériaux de Strasbourg, UMR 7504.
[§] E-mail: daniel.guillon@ipcms.u-strasbg.fr.
[⊥] Fax and phone: (+) 34 976 761209. E-mail: joseluis@unizar.es.

10.1021/ma030223k CCC: $25.00
Published on Web 10/03/2003

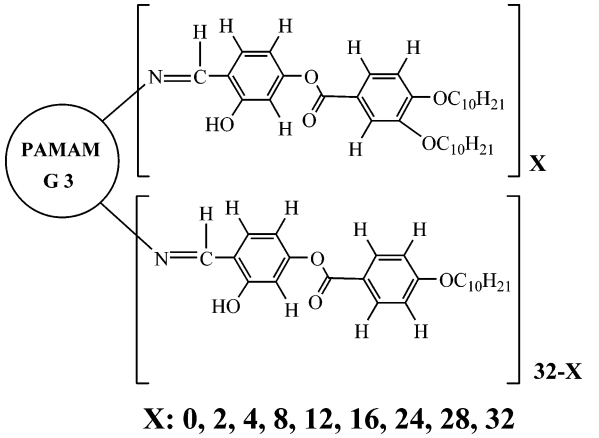

Figure 1. Schematic representation of the codendrimers. *X* is equal to the number of promesogenic units L_2.

codendrimers which have 32 mesogenic units functionalized by one chain (L_1) or two chain (L_2) promesogenic units in various proportions L_1/L_2 (100/0, 94/6, 87.5/12.5, 75/25, 62.5/37.5, 50/50, 25/75, 12.5/87.5 and 0/100) (Figure 1).

The regular variation of the comonomer ratio was thought to smoothly modify the density of aliphatic chains at the outer surface of the dendrimers, forcing the dendrimer to adopt constrained conformations. In this way, the mesomorphic behavior of the corresponding liquid crystalline codendrimers was expected to change from smectic phases to columnar mesophases. The different mesomorphic structures are explained in view of the necessary molecular arrangement adopted by the mesogenic units as a function of the total number of aliphatic chains in one single dendritic molecule.

Results and Discussion

Synthesis. All the dendrimers were synthesized by condensation reactions between the terminal amino groups of third generation PAMAM dendrimer and the aldehyde function of the peripheral units, which consisted of well-defined mixtures of 4-(4′-decyloxybenzoyloxy)salicylaldehyde (L_1) and 4-(3′,4′-didecyloxybenzoyloxy)salicylaldehyde (L_2) in various proportions. As it will be seen in the characterization section, the promesogenic units L_1 and L_2 are statistically distributed around the dendrimer core, essentially due to their similar reactivity with the dendritic core, both in terms of position and number as determined by the initial ratio of L_1/L_2. Isolated as air-stable yellow solids, the compounds are soluble in dichloromethane, chloroform, THF, and insoluble in ethanol.

Characterization. The chemical structures of the compounds were established on the basis of ^{1}H, ^{13}C NMR, IR spectroscopy, and elemental analysis. All these techniques gave satisfactory results.

IR, ^{1}H NMR, and ^{13}C NMR spectroscopic techniques have proved very useful in confirming the structure and the purity of these materials. In addition, the excellent solubility of these dendrimers in $CDCl_3$ allowed us to confirm in all cases that the expected dendrimers were obtained. Evidence of the condensation reaction was provided by the lack of a signal at $\delta = 192$ in the ^{13}C NMR spectra (which corresponds to the carbonyl of the aldehyde) along with the total absence of the NH_2 signals from the starting compound in ^{1}H NMR and IR spectra.

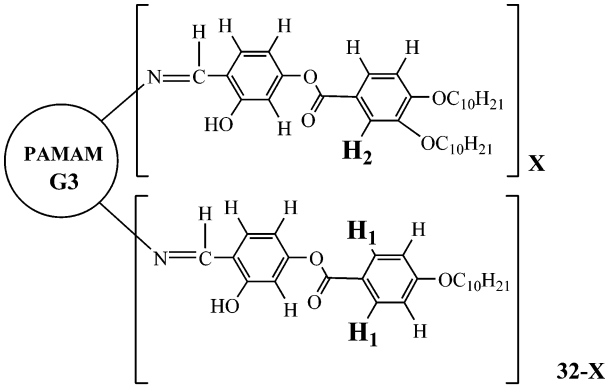

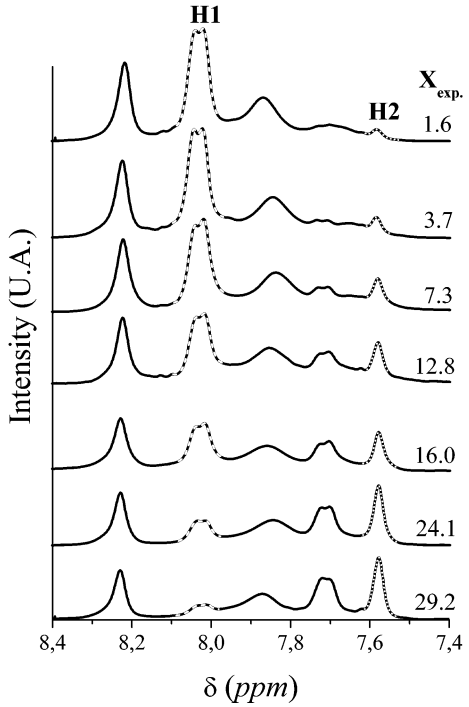

Figure 2. Evolution of the H1 (short dash) and H2 (short dot) proton NMR peaks in the PAMAM codendrimers series. Experimental value of *X* (X_{expt}) were added.

^{1}H NMR was used for the determination of the average number of L_1 and L_2 present in a given codendrimer. As a matter of fact the benzoyloxy moiety of the promesogenic unit L_1 gives rise to an AA′XX′ spin system in the proton NMR spectrum with the two resultant resonances centered at 8.12 ppm (H1) and 6.98 ppm (Figure 2). In contrast, the benzoyloxy moiety of the promesogenic unit L_2 gives rise to three distinct proton resonances at 6.94 ppm, 7.62 ppm (H2), and 7.80 ppm. Therefore, by comparing the integration of the proton NMR signals of H1 and H2 to the theoretical ratio of promesogenic units L_1 and L_2, it was possible to determine the average relative concentration of each promesogenic unit in a given codendrimer.[6] Experimental values of L_1 and L_2 determined by this method are presented in Table 1. Furthermore, the representation of the whole ^{1}H NMR spectrum in the benzene ring area clearly shows the increase (respectively the decrease) of the intensity of the resonance peak associated with H2 (H1) in proportion of the number of promesogenic units L_2 (L_1) present in a given codendrimer (Figure 2).

As can be seen, good agreement between the experimental and theoretical values is obtained confirming the

Table 1. Experimental and Theoretical Number of Promesogenic Units L_1 and L_2 Determined by ^{1}H NMR

	L_1			L_2		
codendrimer	expt	%	theor	expt	%	theor
PAMAM(L_1)30(L_2)2	30.4	95.0	30	1.6	5.0	2
PAMAM(L_1)28(L_2)4	28.3	88.4	28	3.7	11.6	4
PAMAM(L_1)24(L_2)8	24.7	77.2	24	7.3	22.8	8
PAMAM(L_1)20(L_2)12	19.2	60.0	20	12.8	40	12
PAMAM(L_1)16(L_2)16	16.0	50.0	16	16.0	50	16
PAMAM(L_1)8(L_2)24	7.9	24.7	8	24.1	75.3	24
PAMAM(L_1)4(L_2)28	2.8	8.8	4	29.2	91.2	28

similar reactivity of the two comonomers in the condensation reaction. HPLC chromatograms obtained for each compound of the series reflect this statistical distribution of the codendrimers by exhibiting broad peaks containing a maximum centered on the desired compound.

Thermal and Mesomorphic Behavior. Decomposition of these materials was found by thermogravimetric analysis to occur at around 200°C. To avoid any decomposition of the compounds all the thermal and thermodynamic studies were performed below this temperature.

The liquid crystalline properties of these codendrimers were studied by polarizing optical microscopy (POM), differential scanning calorimetry (DSC), and X-ray diffraction (XRD). The thermal and thermodynamic data of the PAMAM(L_1)32−X(L_2)X dendrimers are summarized in Table 2. The phase behavior of these materials is presented in Figure 3.

As previously reported, the dendrimers fully functionalized with either promesogenic units L_1 (bearing one terminal chain) or L_2 (bearing two terminal chains) exhibit only one mesophase, namely a SmA or a Col_h phase respectively, whereas all the new codendrimers exhibit polymorphism depending on the relative proportions of L_1 and L_2. In addition to the SmA phase, the codendrimers exhibit a low-temperature SmC phase ($X = 2$, 4, 8, 12) or a Col_r phase when $X = 16$, 24; the codendrimer with $X = 28$ exhibits both Col_r and Col_h phases.

These codendrimers present very simple DSC thermograms during the first heating scan. They exhibit a glass-to-mesophase transition at T_g, a mesophase-to-mesophase transition at T_{mes}, and a mesophase-to-isotropic liquid transition at T_i (Figure 4). The values of T_g and T_{mes} are given from the second heating scan when the first heating scan was stopped just below the isotropic temperature. The latter is given from the last heating scan. For all the codendrimers, the temperature of the mesophase−mesophase transition decreases slightly as a function of the number of heating runs. This behavior can be explained in terms of a rearrangement of the molecular conformation that takes place at high temperature, and in some extent to some degree of polymolecularity. Indeed, the high proportion of the soft part in these molecules (central dendritic network and peripheral chains) allows for a high conformational freedom that would account for a statistic redistribution of the collection of shapes and hence the adoption of either a pronounced globular conformation or a flattened shape during these successive thermal treatments.

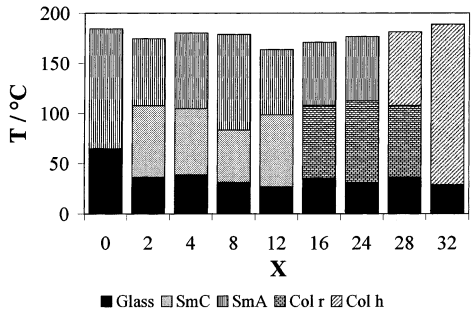

Figure 3. Phase behavior of the PAMAM(L_1)32−X(L_2)X (the thermal data of the previous described homodendrimers have been included).

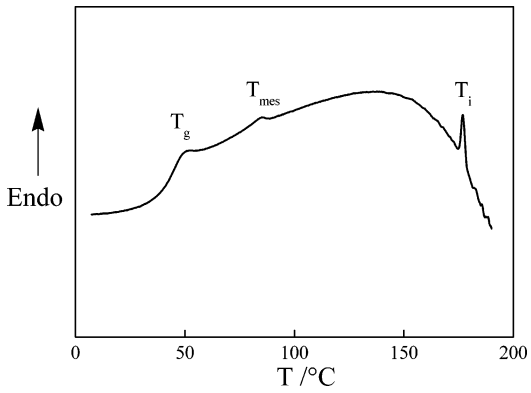

Figure 4. DSC curve corresponding to the fourth heating scan of the codendrimer PAMAM(L_1)28(L_2)4.

Moreover, the variation of ΔS as a function of the experimental number of L_2 (Figure 5) deserves some comments. A regular decrease of the entropy values is observed at the SmC to SmA and SmA to I transitions when the proportion of L_2 increases. This seems to indicate a destabilization of the lamellar phases when the number of aliphatic chains on the outer surface of the codendrimer increases, pointing to a decrease in the interactions between the dendrimeric molecules. Similarly, the entropies of Col_h to I and Col_r to SmA transitions decrease when the proportion of L_1 increases, pointing to a destabilization of the columnar structure.

X-ray Diffraction Studies. The nature of the mesophases was determined by X-ray diffraction (XRD), as a function of temperature. For this study, the samples

Table 2. Thermal (T^c) and Thermodynamic Data (ΔH^d) for the PAMAM(L_1)32−X(L_2)X Codendrimers Series

	g		Col_r			Col_h			SmC			SmA			I
PAMAM(L_1)30(L_2)2	•	36.5[a]							•	108.0[a]	(14.0)	•	174.7[b]	(16.5)	•
PAMAM(L_1)28(L_2)4	•	38.9[a]							•	105.0[a]	(14.4)	•	180.4[b]	(13.4)	•
PAMAM(L_1)24(L_2)8	•	31.5[a]							•	83.7[a]	(10.1)	•	178.9[b]	(13.0)	•
PAMAM(L_1)20(L_2)12	•	27.0[a]							•	98.9[a]	(7.2)	•	163.7[b]	(12.2)	•
PAMAM(L_1)16(L_2)16	•	35.5[a]	•	108.2[a]	(11.9)							•	171.0[b]	(10.6)	•
PAMAM(L_1)8(L_2)24	•	31.1[a]	•	112.7[a]	(16.8)							•	176.7[b]	(8.8)	•
PAMAM(L_1)4(L_2)28	•	36.1[a]	•	107.9[a]	(14.4)	•	181.4[b]	(12.5)							•

[a] Data correspond to the second heating scan of initial sample without reaching the isotropic temperature [b] Data correspond to the first heating scan of a different sample reaching the isotropic temperature. [c] Temperatures (°C) of the mesophase transition and isotropic point are taken at the maximum of the peaks. [d] Value of ΔH from the phase transition (in J mol^{-1}. K^{-1}) are put in parentheses near the corresponding temperature.

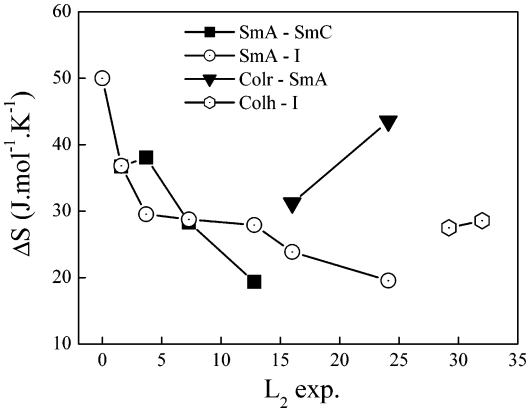

Figure 5. Variation of the entropy ΔS as a function of number of promesogenic unit L_2.

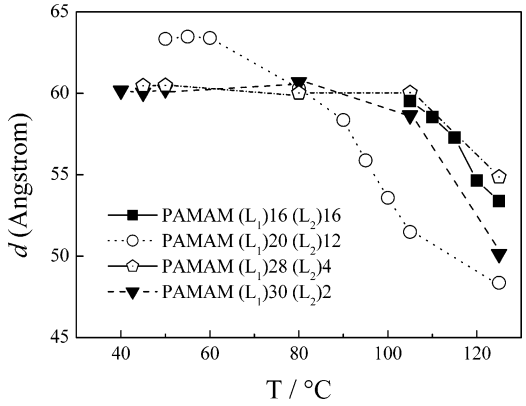

Figure 6. Variation of the inter lamellar spacing *d* as a function of temperature for the PAMAM codendrimers.

were loaded into Lindemann glass capillaries and irradiated at room-temperature both in the virgin state and after a thermal treatment consisting of heating the sample to a temperature at which it is fluid, annealing at this temperature for a few minutes, and then cooling. In addition to this, high-temperature experiments were also carried out.

Before the detailed analysis of the different types of mesophases obtained is given, let us remark that the mesomorphic organizations (lamellar or columnar) were retained at room temperature in the glassy state for all the dendrimers. The existence of smectic mesophases was easily confirmed by the presence of a set of (at least) two equally spaced maxima (reciprocal spacings in the ratio 1:2) in the low-angle region of the X-ray patterns. In contrast to the general behavior observed in classical low-molecular-weight liquid crystals in which the layer spacing is larger in the SmA than in the SmC mesophase, the opposite behavior was found in this series (as in other series of dendrimers previously reported[4c]) (see Figure 6). The hexagonal columnar mesophase was identified by the presence of a set of three sharp reflections in the ratio $1:\sqrt{3}:\sqrt{4}$ in the low-angle region of the X-ray patterns. As for the rectangular columnar mesophase, a more complex pattern was systematically obtained including two small-angle fundamental reflections as well as some additional higher order reflections that were indexed according to a two-dimensional rectangular lattice. In addition, all the X-ray patterns of the smectic and of the columnar mesophases contain in the wide-angle region a broad, diffuse halo characteristic of the conformationally disordered aliphatic chains. The types of mesophases determined for each

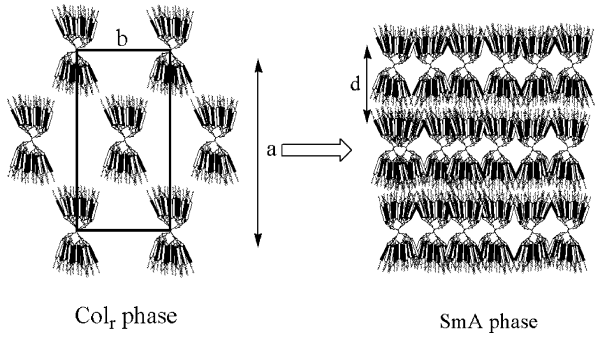

Figure 7. Schematic representation of the transition from the columnar rectangular mesophase to the lamellar smectic A mesophase exhibited by codendrimers containing intermediate numbers of L_2 units ($X = 16, 24, 28$).

compound by the combination of texture observations and X-ray diffraction are represented in Figure 3, and the deduced structural parameters are given in Table 3.

It is worth noting that in all cases the layer spacing (*d* paramenter in Table 3) is significantly smaller than the moleculer length estimated from its most stretched conformation. This is not unexpected, and the same phenomenon is generally observed in classical calamitic liquid crystals as a consequence of the disorder of the hydrocarbon chains. In the case of dendrimers this behavior is even more marked, because not only the terminal hydrocarbon chains but also the central dendrimer cores are highly disordered. As far as the rectangular columnar mesophases are concerned, the *a* lattice parameter is in the three cases much larger than the *b* parameter (Table 3). Furthermore, for the two compounds that show both smectic A and rectangular columnar mesophases, the value of the rectangular lattice parameter *a* is about twice the value of the smectic spacing *d*. To account for this behavior, we must assume that the molecules are packed in the columnar mesophase with the mesogenic units and the terminal hydrocarbon chains elongated mainly along the *a* axis. The molecules located at the center and at the corners of the unit cell, are arranged in such a way that the chains of two molecules (one at the center and another one at a corner) are not interdigitated but are only in contact via their terminal methyl groups. Thus, each molecule occupies a length of *a*/2 (see Figure 7). Such a rectangular columnar mesophase corresponds to a two-dimensional arrangement of parallel columns where the terminal hydrocarbon chains segregate in layers. At the transition to the smectic A mesophase the correlation along the columnar axis is lost, leading to the disruption of the two-dimensional positional ordering so that the columnar order is destroyed generating a lamellar system. This description of the columnar-to-smectic mesophase transition is consistent with what has been observed in other liquid crystalline systems with complex morphologies.[7]

It is worth mentioning, that for each compound and for a particular mesophase the structural parameters depend not only on the temperature (see Figure 6) but also on the thermal history. Indeed, when several X-ray patterns are taken at a constant temperature, a decrease in the layer spacing is clearly observed, particularly in the SmA phase. For example, *d* in the smectic A phase of PAMAM(L_1)16(L_2)16 is initially 57 Å at 125°C, but decreases down to 54 Å when the sample is maintained at this temperature for 2 h, and is found to

Table 3. X-ray Results for the Mesophases of Compounds in the Series PAMAM(L_1)32−*X*(L_2)*X*[c]

compound	*T* (°C)	M	*h k l*[a]	d_{obsd} (Å)	d_{calcd} (Å)	lattice constants (Å)[a]
PAMAM(L_1)$_{28}$(L_2)$_4$	25	SmC	0 0 1	59.6	60.0	$d = 60$
			0 0 2	30.2	30.0	
				4.4[b]		
	55	SmC	0 0 1	59.6	59.5	$d = 59.5$
			0 0 2	29.6	29.75	
				4.4[b]		
	125	SmA	0 0 1	54.8	55.0	$d = 55$
			0 0 2	27.9	27.5	
				4.6[b]		
PAMAM(L_1)$_{24}$(L_2)$_8$	25	SmC	0 0 1	60.4	60.0	$d = 60$
			0 0 2	30.2	30.0	
				4.3[b]		
	60	SmC	0 0 1	59.6	60.0	$d = 60$
			0 0 2	30.1	30.0	
				4.4[b]		
	115	SmA	0 0 1	57.8	58.0	$d = 58$
			0 0 2	29.4	29.0	
				4.6[b]		
PAMAM(L_1)$_{20}$(L_2)$_{12}$	25	SmC	0 0 1	61.0	61.0	$d = 61$
			0 0 2	30.8	30.5	
				4.3[b]		
	80	SmC	0 0 1	60.0	60.5	$d = 60.5$
			0 0 2	30.8	30.25	
				4.4[b]		
	92	SmA	0 0 1	59.2	59.5	$d = 59.5$
			0 0 2	29.8	29.75	
				4.5[b]		
	105	SmA	0 0 1	54.0	54.0	$d = 54$
			0 0 2	27.1	27.1	
				4.6[b]		
PAMAM(L_1)$_{16}$(L_2)$_{16}$	80	Col_{rec}	2 0	59.9	59.9	$a = 119.8$
			1 1	49.6	49.6	$b = 54.5$
			3 1	31.9	32.2	
			4 0	29.5	29.95	
				4.4[b]		
	125	SmA	0 0 1	56.9	57.0	$d = 57$
			0 0 2	28.5	28.5	
				4.6[b]		
PAMAM(L_1)$_8$(L_2)$_{24}$	100	Col_{rec}	2 0	57.5	57.5	$a = 115$
			1 1	42.6	42.6	$b = 46$
			3 1	30.0	29.4	
			4 0	28.75	28.75	
				4.3[b]		
	135	SmA	0 0 1	53.5	54.0	$d = 54$
			0 0 2	27.5	27.0	
				4.6[b]		
PAMAM(L_1)$_4$(L_2)$_{28}$	75	Col_{rec}	2 0	52.1	52.1	$a = 104.2$
			1 1	45.1	45.1	$b = 50$
			3 1	28.1	28.5	
			4 0	25.5	26.0	
				4.4[b]		
	125	Col_{hex}	1 0	53.6	53.7	$a = 62.3$
			1 1	31.6	31.0	
			2 0	26.8	26.8	
				4.5[b]		
	140	Col_{hex}	1 0	46.8	46.8	$a = 54$

[a] *d*, layer spacing; *a*, *b*, rectangular or hexagonal lattice constants; *h*, *k*, *l*, Miller indices. [b] Broad, diffuse maximum. [c] In each column of the table are listed, respectively, the compound code, the temperature of the experiment, the type of mesophase, the proposed indexation, the observed and calculated spacings, and the lattice constants.

be 52 Å after 4 h at the same temperature. Indeed, the data represented in Figure 6 were obtained from a study performed on increasing temperature with an exposure time of about 1 h for each temperature. For example, the layer thickness of PAMAM(L_1)16(L_2)16 represented in Figure 6 is 53.5 Å at 125 °C, whereas it is 57 Å when the sample was heated directly to that temperature. This phenomenon is probably connected with the above-mentioned variation of the transition temperatures as a function of the number of DSC scans. A tentative explanation would be a change of the central dendritic conformation when the materials are heated in the highest temperature range of the mesophases consequent to a redistribution of the terminal branches in space. This would result in a more flattened shape of the central dendrimer core due to an enhanced conformational disorder. In the same way, this could explain the smaller layer thickness of the SmA compared to the SmC mesophase, an argument that together with the orientational fluctuations of the mesogenic units was used to account for the same phenomenon in a previous series of DAB dendrimers.[4c]

For useful comparisons, only the initial data (obtained from short-exposure-time patterns) are presented in Table 3. For the same reason, for the low-temperarature mesophases, in which the effect of the temperature and of the time is not significant, the data obtained at room temperature are given in some cases. In fact, in the SmC and in the Col_r mesophases, the spacings measured at room temperature do not change after the thermal treatment mentioned at the begining of this section, and they do not change significantly with increasing temperature until the mesophase−mesophase transition (see the SmC spacing of compounds PAMAM(L_1)28(L_2)4,

PAMAM(L_1)24(L_2)8 and PAMAM(L_1)20(L_2)12 in Table 3).

Supramolecular Organization in the Mesophase. Thus, from a general point of view, a change of mesophase structure was achieved by a simple molecular approach (Figure 3), and such an evolution was found to occur in a multiple-step process upon increasing the content of the two-chained component, i.e., a dependence on the relative proportions of promesogenic units L_1 and L_2 and therefore on the number of alkoxy chains present around the dendritic core. As could have been expected, columnar mesophases, whatever their 2D symmetry (hexagonal or rectangular), are observed for L_2-rich dendrimers, i.e., when at least half of the branches are substituted with L_2 ($X \geq 16$). On the other hand, smectic mesophases (SmA and SmC) are stable over a broad concentration range, and are still observed for dendrimers containing a relatively high content of L_2 units ($0 \leq X \leq 24$). Both lamellar and columnar structures coexist for intermediate numbers of L_2 units ($16 \leq X \leq 24$) as a function of temperature. These changes are clearly related to the increase in the average number of peripheral chains around the dendrimer, i.e., the modification of the aliphatic/aromatic interfacial curvature; hence, such a behavior is reminiscent of lyotropic systems where one of the chemical constituents of an amphiphile increases its area in contact with a solvent having a similar polarity. In this case, the chains can be considered as the solvent but directly linked to the molecule, and thus the situation differs quite substantially from purely lyotropic materials. In other words, the so-called solvent acts more as a diluent or as a swelling agent and is not a prerequisite condition for mesophase formation. However, this is another original illustration of the concept of internal solvent.

As it was shown previously,dendrimers functionalized with promesogenic units containing only one decyloxy chain form thick rods or cylinders which are further organized into a lamellar SmA mesophase. This behavior was described by a model based on the spatial segregation of the various constitutive parts: the promesogenic units are aligned more or less parallel to each other and extended up and down from the dendritic core, with a good segregation between the aliphatic and aromatic parts. Incorporation of small amounts of the promesogenic unit L_2 ($X < 16$) in the dendrimers stabilized the SmC phase at low temperature and the SmA phase at high temperature. The presence of additional chains will slightly disturb this subtle equilibrium, and in order to accommodate these extra chains, the anisometric rigid cores will tilt so that the cross sectional area of the cylinder is increased. Hence, the SmC phase is formed, contrary to the case of the homodendrimers with a single-chain mesogenic unit where it is not observed. At higher temperature a SmA mesophase appears due to the increasing molecular disorder within the layer planes, and to the higher conformation freedom of the alkoxy chains and dendrimer core (the molecular area is indeed increased). This phenomenon is likely accompanied by a random tilt of the aromatic segments of the molecule with respect to the normal of the layer plane which occur with local fluctuation of the tilt angle and orientation (i.e. there is no long-range correlation of the tilt angle and the tilt plane). Presumably, this behavior could be correlated to the breaking of the H-bonding of the dendritic core.

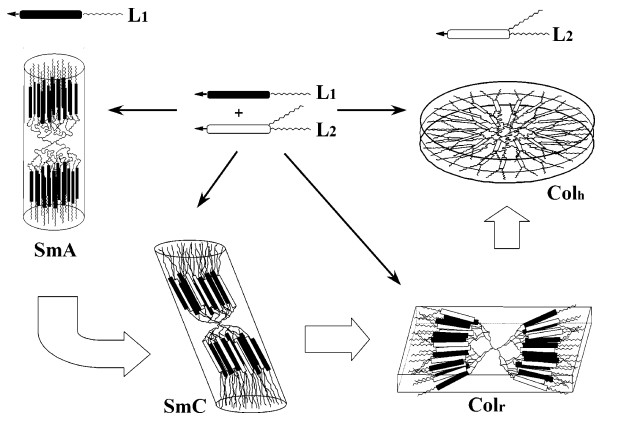

Figure 8. Lamellar to columnar evolution as a function of the number of promesogenic units L_1 and L_2.

When the number of promesogenic units L_2 is equal to or higher than L_1 ($X \geq 16$), all the compounds exhibit a columnar mesophase which is rectangular or hexagonal depending on both the number of promesogenic units L_2 and the temperature. Of particular interest here is the Col_r phase that exists either below the SmA phase ($X = 16, 24$) or below the Col_h phase ($X = 28$). This mesophase clearly plays a pivotal role in the transition between the lamellar and columnar regimes. To try to explain the occurrence of these two mesophases, let us consider the space occupied around the dendrimer core by the alkoxy chains. Usually, in such types of liquid crystal dendrimers,[4a] a high density of aliphatic chains imposes a curved interface between the promesogenic units and the paraffinic chains. This forces the dendritic core to change its spatial conformation from oblate to prolate; i.e. the thick rod conformation evolves toward a more flattened conformation and hence from a lamellar to a columnar structure. These deformations could be followed almost stepwise due to the incremental increase of the chain density around the dendrimer.

For PAMAM(L_1)4(L_2)28, the Col_r to Col_h transition is explained by a temperature effect, which provides an higher degree of freedom to the alkoxy chains, and by the number of chains, which is less than the homodendrimer fully substituted by L_2 mesogenic units. The large number of chains is sufficient to force the dendrimer to squeeze or flatten (Figure 8), and to generate columnar self-assembling as explained previously.[4c] However, due to the slight deficit of chains compared to the pure homodendrimer containing only L_2 units, the chains are not distributed homogeneously around the dendritic core but are distributed along preferred directions as the temperature was lowered. This semiradial molecular conformation leads also to a self-assembling process into columns, but with a noncircular columnar cross section, and thus to the preferential formation of a Col_r mesophase. Reducing the number of L_2 units at the expense of L_1 units ($X = 16, 24$) first is sufficient to totally suppress the Col_h phase but not the columnar mesomorphism, confirming the above assumptions. It is also sufficient to allow stabilization of the SmA phase as the temperature is increased. Though one cannot give a clear explanation of this columnar to smectic transition process, it is clear that a subtle change of chain density has a strong influence on the molecular conformation and the consequent packing and organization within a mesophase. The Col_r phase plays an essential role as an intermediate phase

that can accommodate such molecular distortions into a perfectly stable arrangement.

Conclusions

In this paper we have shown that it is possible to synthesize liquid crystal codendrimers which contain a very well-defined ratio of two different kinds of promesogenic unit. The characterization of these molecules with high molecular weight was undertaken by a combination of different techniques such as, elemental analysis, infrared spectroscopy, and proton and carbon NMR. NMR appeared to be very useful to determine the average number of each kind of promesogenic units per dendrimer. X-ray diffraction studies have permitted to follow the mesomorphic behavior of these compounds as a function of temperature and composition, from non tilted lamellar mesophase to hexagonal columnar mesophase passing through tilted smectic and rectangular columnar mesophases. This study has enabled us to confirm that the mesomorphic behavior of such block molecules could be modulated and controlled by a simple modification of the ratio of two promesogenic units present around the dendrimer core. According to these results we have shown that it is possible to synthesize codendrimers molecules "à la carte" exhibiting a predictable liquid crystalline behavior.

Experimental Section

Techniques. Microanalyses were performed with a Perkin-Elmer 240B microanalyzer. Infrared spectra were obtained with a Perkin-Elmer 1600 (FTIR) spectrophotometer in the range $\tilde{\nu} = 400-4000$ cm^{-1} spectral range. ^{1}H and ^{13}C NMR spectra were recorded on a Varian Unity 300 MHz spectrometer in $CDCl_3$ solutions. The optical textures of the mesophases were studied with a Nikon polarizing microscope equipped with a Mettler FP8 hot-stage and an FP80 central processor. The transition temperatures and enthalpies were measured by differential scanning calorimetry with a Perkin-Elmer DSC-7 instrument operated at a scanning rate of 10 °C min^{-1} on heating and cooling. The apparatus was calibrated with indium (156.6 °C; 28.4 J g^{-1}) as the standard. Thermogravimetric experiments were performed using a TA instruments SDT 2960 simultaneous DTA-TGA (heating rate 10 °C/min; air stream). The XRD patterns were obtained with two different experimental setups. In the first set, XRD measurements were performed with a pinhole camera (Anton-Paar) operating with a point-focused Ni-filtered Cu Kα beam. The sample was held in Lindemann glass capillaries (1 mm diameter) and heated, when necessary, with a variable-temperature oven. The patterns were collected on flat photographic films. The capillary axis and the film are perpendicular to the X-ray beam. Spacings were obtained via Bragg's law. In the second set the XRD patterns were obtained with a Debye−Scherrer camera equipped with a bent quartz monochromator, and a homemade oven. The crude powder was filled in Lindemann capillaries of 1 mm diameter. The diffraction patterns were recorded with a curved Inel CPS 120 counter gas-filled detector linked to a data acquisition computer; periodicities up to 60 Å can be measured and the sample temperature controlled to within ±0.05 °C.

General Procedure for the Synthesis of Liquid Crystalline Codendrimers. Neutral activated grade I alumina (0.6 g) and the third generation poly(amidoamine) dendrimer was added, under argon, to a stirred solution of 4-(4′-decyloxybenzoyloxy)salicylaldehyde and 4-(3′,4′-didecyloxybenzoyloxy)salicylaldehyde (in desired ratio L_1:L_2) in CH_2Cl_2 (75 mL). After one night, the alumina was filtered off and the solvent evaporated from the filtrate under vacuum. The yellow product was dissolved in hexane and purified by column chromatography (CH_2Cl_2/Hexane 1:2). Yields: 70−85%.

Characterization. These materials exhibit similar ^{1}H and ^{13}C NMR spectra. The data of the PAMAM $(L_1)16(L_2)16$ codendrimer only are reported as a representative example. Moreover, due to the complexity of the ^{1}H NMR spectrum of this codendrimer (broad picks), it was not possible to describe it totally both in term of integration and peaks coupling. For this reason, the chemical shift of each peak of the spectrum is given. The data obtained from other techniques have been reported for all the compounds of the series.

PAMAM$(L_1)4(L_2)28$. IR (Nujol): $\tilde{\nu}$ = 3387, 3290 (CON−H), 1728 (OC═O), 1658 (sh HN−C═O), 1638 cm^{-1} (CH═N). Anal. Calcd for $C_{1348}H_{2060}N_{122}O_{216}$ (23431.5): C, 69.10; H, 8.86; N, 7.29. Found: C, 68.47; H, 9.10; N, 7.10.

PAMAM$(L_1)8(L_2)24$. IR (Nujol): $\tilde{\nu}$ = 3375, 3300 (CON−H), 1727 (OC═O), 1656 cm^{-1} (sh HN−C═O), 1634 cm^{-1} (CH═N). Anal. Calcd for $C_{1310}H_{1984}N_{122}O_{212}$ (22835.16): C, 68.90; H, 8.76; N, 7.48. Found: C, 68.86; H, 8.74; N, 7.42.

PAMAM$(L_1)16(L_2)16$. ^{1}H NMR (300 MHz, $CDCl_3$): δ = 13.8, 8.21, 8.02, 7.99, 7.84, 7.71, 7.68, 7.56, 7.14, 7.12, 6.88, 6.86, 6.63, 6.57, 6.54, 3.98, 3.62, 3.45, 3.19, 2.67, 2.47, 2.29, 1.78, 1.76, 1.41, 1.23, 0.85, 0.84.

^{13}C NMR (300 MHz, $CDCl_3$): δ = 173.08, 172.61, 165.77, 164.57, 163.99, 163.65, 154.57, 153.96, 148.68, 132.71, 132.29, 124.49, 121.74, 121.09, 116.24, 114.59, 114.31, 112.09, 111.93, 110.67, 69.33, 69.03, 68.32, 57.36, 52.33, 50.15, 40.00, 33.99, 31.87, 29.54, 29.39, 29.32, 29.21, 29.08, 26.02, 25.96, 22.64, 14.06. IR (Nujol): $\tilde{\nu}$ = 3402, 3287 (CON−H), 1728 (OC═O), 1658 (sh HN−C═O), 1637 cm^{-1} (CH═N). Anal. Calcd for $C_{1230}H_{1824}N_{122}O_{204}$ (21584.3): C, 68.44; H, 8.52; N, 7.92. Found: C, 67.99; H, 8.43; N, 7.57.

PAMAM$(L_1)20(L_2)12$. IR (Nujol): $\tilde{\nu}$ = 3364, 3284 (CON−H), 1729 (OC═O), 1662 (sh HN−C═O), 1638 cm^{-1} (CH═N). Anal. Calcd for $C_{1189}H_{1744}N_{122}O_{200}$ (20947.27): C, 68.17; H, 8.39; N, 8.16. Found: C, 67.93; H, 8.59; N, 7.83.

PAMAM$(L_1)24(L_2)8$. IR (Nujol): $\tilde{\nu}$ = 3403, 3306 (CON−H), 1726 (OC═O), 1657 (sh HN−C═O), 1634 cm^{-1} (CH═N). Anal. Calcd for $C_{1150}H_{1664}N_{122}O_{196}$ (20334.84): C, 67.93; H, 8.25; N, 8.40. Found: C, 67.65; H, 8.81; N, 8.30.

PAMAM$(L_1)28(L_2)4$. IR (Nujol): $\tilde{\nu}$ = 3396, 3275 (CON−H), 1729 (OC═O), 1655 (sh HN−C═O), 1639 cm^{-1} (CH═N). Anal. Calcd for $C_{1110}H_{1584}N_{122}O_{192}$ (19709.16): C, 67.64; H, 8.10; N, 8.67. Found: C, 67.36; H, 8.55; N, 8.49.

PAMAM$(L_1)30(L_2)2$. IR (Nujol): $\tilde{\nu}$ = 3405, 3282 (CON−H), 1729 (OC═O), 1658 (sh HN−C═O), 1637 cm^{-1} (CH═N). Anal. Calcd for $C_{1099}H_{1564}N_{122}O_{191}$ (19540.89): C, 67.50; H, 8.07; N, 8.74. Found: C, 66.96; H, 8.42; N, 8.53.

Acknowledgment. This work was supported by the RTN Project Supramolecular Liquid Crystal Dendrimers (LCDD) from the European Union (HPRN-CT2000-00016) and by the Comisión Interministerial de Ciencia y Tecnología (Spain) (Projects MAT2000-1293-C02-01 and MAT2002-04118-C02-01).

References and Notes

(1) (a) Tomalia, D. A.; Naylor, A. M.; Goddard, W. A., III. *Angew. Chem., Int. Ed. Engl.* **1990**, *29*, 138−175. (b) Issberner, J.; Moors, R.; Vögtle, F. *Angew. Chem., Int. Ed. Engl.* **1994**, *33*, 2413−2420. (c) Ardouin, N.; Astruc, D. *Bull. Soc. Chem. Fr.* **1995**, *132*, 875−909. (d) Newkome, G. R.; Moorefield, C. N.; Vögtle, F. In *Dendritic Molecules: Concepts, Synthesis and Perspectives*; VCH: Weinheim, Germany, 1996. (e) Ashton, P. R.; Boyd, S. E.; Brown, C. L.; Nepogodiev, S. A.; Meijer, E. W.; Peerlings, H. W. I.; Stoddart, J. F. *Chem.—Eur. J.* **1997**, *3*, 974−984. (f) Zeng, F.; Zimmerman, S. C. *Chem. Rev.* **1997**, *97*, 1681−1712. (g) Matthews, O. A.; N. Shipway, N.; Stoddart, J. F. *Prog. Polym. Sci.* **1998**, *23*, 1−56. (h) Chow, H. F.; Mong, T. K. K.; Nongrum, M. F.; Wan C. W. *Tetrahedron* **1998**, *54*, 8543−8660. (i) Fischer, M.; Vögtle, F. *Angew. Chem., Int. Ed.* **1999**, *38*, 884−905. (j) Inoue, K. *Prog. Polym. Sci.* **2000**, *25*, 453−571.

(2) (a) Ponomarenko, S. A.; Boiko, N. I.; Shibaev, V. P. *Polym. Sci., Ser. C* **2001**, *33*, 1−45 and references therein. (b) Bobrovsky, A.Yu; Pakhomov, A. A.; Zhu, X. M.; Boiko, N. I.; Shibaev, V. P.; Stumpe, J. *J. Phys. Chem. B* **2002**, *106*, 540−546. (c) Bobrovsky, A. Yu; Ponomarenko, S.; Boiko, N. I.; Shibaev, V.; Rebrov, E.; Muzafarov, A.; Stumpe, J.; *J.*

Macromol. Chem. Phys. **2002**, *203*, 1539−1546. (d) Saez, I. M.; Goodby, J. W.; Richardson, R. M. *Chem.−Eur. J.* **2001**, *7*, 2758−2764. (e) Elsässer, R.; Melh, G. H.; Goodby, J. W.; Veith, M.; *Angew. Chem., Int. Ed.* **2001**, *40*, 2688−2690. (f) Tsiourvas, D.; Stathopoulu, K.; Sideratou, Z.; Paleos, C. M.; *Macromolecules* **2002**, *35*, 1746−1750. (g) Tsiourvas, D.; Felekis, T.; Sideratou, Z.; Paleos, M. C. *Macromolecules* **2002**, *35*, 6466−6469. (h) Dautlgraber, G.; Baumeister, V.; Diele, S.; Kresse, H.; Luhmann, B.; Lang, H.; Tschierske, C. *J. Am. Chem. Soc.* **2002**, *124*, 14852−14853. (i) Buzón, P.; Örtegren, J.; Ihre, H.; Gedde, U. W.; Hult, A.; Andersson, G.; Eriksson, A.; Lindgren, M. *Macromolecules* **2002**, *35*, 1663−1671.

(3) Barberá, J.; Marcos, M.; Serrano, J. L. *Chem.−Eur. J.* **1999**, *5*, 1834−1840. Percec, V.; Kawasumi, M. *Macromolecules* **1992**, *25*, 3843−3850. Percec, V.; Cho, C. G.; Pugh, C.; Tomazos, D. *Macromolecules* **1992**, *25*, 1164−1176. Percec, V.; Chu, P.; Ungar, G.; Zhou, J. *J. Am. Chem. Soc.* **1995**, *117*, 11441−11454. Percec, V.; Johansson, G.; Ungar, G.; Zhou, J.; *J. Am. Chem. Soc.* **1996**, *118*, 9855−9866. Balagurusamy, V. S. K.; Ungar, G.; Percec, V.; Johansson, G. *J. Am. Chem. Soc.* **1997**, *119*, 1539−1555. Percec, V.; Cho, W. D.; Ungar, G.; Yeardley, D. J. P. *J. Am. Chem. Soc.* **2001**, *123*, 1302−1315. Percec, V.; Ahn, C.-H.; Ungar, G.; Yeardley, D. J. P.; Möller, M.; Sheiko, S. S. *Nature*, **1998**, *391*, 161−164. Percec, V.; Glodde, M.; Bera, T. K.; Miura, Y.; Shiyanovskaya, I.; Singer, K. D.; Balagurusamy, V. S. K.; Heiney, P. A.; Schnell, I.; Rapp, A.; Spiess, H.-W.; Hudson, S. D.; Duan, H. *Nature*, **2002**, *419*, 384−387. Hudson, S. D.; Jung, H. T.; Percec, V.; Cho, W. D.; Johansson, G.; Ungar, G.; Balagurusamy, U. S. K. *Science* **1997**, *278*, 449−452. Ungar, G.; Liu, Y.; Zeng, X.; Percec, V.; Cho, W. D. *Science* **2003**, *299*, 1208−1211.

(4) (a) Marcos, M.; Giménez, R.; Serrano, J. L.; Donnio, B.; Heinrich, B.; Guillon, D. *Chem.−Eur. J.* **2001**, *7*, 1006−1013. (b) Barberá, J.; Donnio, B.; Giménez, R.; Guillon, D.; Marcos, M.; Omenat, A.; Serrano, J. L. *J. Mater. Chem.* **2001**, *11*, 2808−2813. (c) Donnio, B.; Barberá, J.; Giménez, R.; Guillon., D.; Marcos, M.; Serrano, J. L. *Macromolecules* **2002**, *35*, 370−381.

(5) Ponamorenko, S. A.; Boiko, N. I.; Shibaev, V. P.; Richardson, R. M.; Whitehouse, I. J.; Rebrov, E. A.; Muzarov, A. M. *Macromolecules* **2000**, *33*, 5549.

(6) Determination of the average number of promesogenic unit L_2 by ^{1}H NMR. The average number of promesogenic unit L_2 was determined through the relation between the experimental ratio ρ of the two integrals H1 and H2

$$\rho = \frac{\int_{\text{peak}} \text{H1}}{\int_{\text{peak}} \text{H2}} \tag{1}$$

and the theoretical ratio of the percentage of L_1 and L_2

$$\frac{\%\text{L}_1}{\%\text{L}_2} = \frac{32 - X}{X} \tag{2}$$

where X is the number of L_2 and $32 - X$ the number of L_1, with $\%\ L_1$ or $\%\ L_2$ equal to:

$$\%\ \text{L}_1 = \frac{32 - X}{32} \times 100 \tag{3}$$

$$\%\ \text{L}_2 = \frac{X}{32} \times 100 \tag{4}$$

From (1) and (2), the following relation is deduced

$$\frac{\%\text{L}_1}{\%\text{L}_2} = \frac{1}{2}\rho \tag{5}$$

which leads to the final relationship

$$\text{X} = \frac{32}{\frac{1}{2}\rho + 1} \tag{6}$$

(7) Tschierske, C. *J. Mater. Chem.* **2001**, *11*, 2647−2671.

MA030223K